

High-efficiency multi-photon boson sampling

Hui Wang^{1,2*}, Yu He^{1,2*}, Yu-Huai Li^{1,2*}, Zu-En Su^{1,2}, Bo Li^{1,2}, He-Liang Huang^{1,2}, Xing Ding^{1,2}, Ming-Cheng Chen^{1,2}, Chang Liu^{1,2}, Jian Qin^{1,2}, Jin-Peng Li^{1,2}, Yu-Ming He^{1,2,3}, Christian Schneider³, Martin Kamp³, Cheng-Zhi Peng^{1,2}, Sven Höfling^{1,3,4}, Chao-Yang Lu^{1,2}, and Jian-Wei Pan^{1,2}

¹ Hefei National Laboratory for Physical Sciences at Microscale and Department of Modern Physics, University of Science and Technology of China, Hefei, Anhui, 230026, China

² CAS-Alibaba Quantum Computing Laboratory, CAS Centre for Excellence in Quantum Information and Quantum Physics, University of Science and Technology of China, China

³ Technische Physik, Physikalisches Institut and Wilhelm Conrad Röntgen-Center for Complex Material Systems, Universität Würzburg, Am Hubland, D-97074 Würzburg, Germany

⁴ SUPA, School of Physics and Astronomy, University of St. Andrews, St. Andrews KY16 9SS, United Kingdom

* These authors contributed equally to this work

Abstract:

Boson sampling is considered as a strong candidate to demonstrate the “quantum computational supremacy” over classical computers. However, previous proof-of-principle experiments suffered from small photon number and low sampling rates owing to the inefficiencies of the single-photon sources and multi-port optical interferometers. Here, we develop two central components for high-performance boson sampling: robust multi-photon interferometers with 99% transmission rate, and actively demultiplexed single-photon sources from a quantum-dot-micropillar with simultaneously high efficiency, purity and indistinguishability. We implement and validate 3-, 4-, and 5-photon boson sampling, and achieve sampling rates of 4.96 kHz, 151 Hz, and 4 Hz, respectively, which are over 24,000 times faster than the previous experiments. Our architecture is feasible to be scaled up to larger number of photons and with higher rate to race against classical computers, and might provide experimental evidence against the *Extended Church-Turing Thesis*.

Quantum computers¹ can in principle solve certain problems faster than classical computers. Despite substantial progress in the past two decades²⁻⁴, building quantum machines that can actually outperform classical computers for some specific tasks—an important milestone termed as “quantum supremacy”—remained challenging. In the quest of demonstrating the “quantum supremacy”, boson sampling, an intermediate (i.e., non-universal) quantum computer model proposed by Aaronson and Arkhipov⁵, has received considerable interest as it requires much less physical resources than building universal optical quantum computers⁶.

A quantum boson-sampling machine can be realized by sending n indistinguishable single photons through a passive m -mode ($m > n$) interferometer, and sampling from the probabilistic output distribution. Mathematically, the probability amplitude of each output outcome is proportional to the permanent of a corresponding $n \times n$ submatrix, which is strongly believed to be intractable because calculating the permanent is a so-called #P-complete complexity problem. Note that, however, boson sampling is itself not a #P-complete problem, i.e., cannot efficiently calculate the matrix permanent. For a specifically defined task of sampling over the entire distribution, it is expected that a sufficiently large quantum boson-sampling machine cannot be efficiently simulated by the classical computers^{5,7,8}. In principle, a large-scale boson-sampling machine would constitute an effective disproof against a foundational tenet in computer science: the *Extended Church-Turing Thesis*, which postulates that all realistic physical systems can be efficiently simulated with a (classical) probabilistic Turing machine.

To this end, an experimental roadmap for demonstrating “quantum supremacy” is to construct multi-photon boson-sampling machines with increasing number of input photons and faster sampling rates to race against classical computers. However, the overall performance of the previous proof-of-principle boson-sampling experiments⁹⁻¹⁷ were critically limited due to the lack of high-quality single-photon sources and low-loss multi-mode circuits. For example, the most commonly used pseudo-single photons created using spontaneous parametric down-conversion¹⁸ (SPDC) were intrinsically probabilistic and mixed with multi-photon components. The SPDC probability was

kept small (about a few percent) in order to suppress the unwanted two-photon emission. The frequency correlation of the SPDC photon pairs and the inefficient collection into single-mode fibers further reduced the single-photon heralding efficiency to typically a low level of $\sim 1\%$ in the previous work⁹⁻¹⁶ (see Supplementary Information Table S1). In addition, the boson-sampling rate was significantly reduced due to the coupling and propagation loss in the multi-mode photonic circuits. In an attempt to solve the intrinsic probabilistic problem of SPDC, spatial or temporal multiplexing^{19,20} and scattershot boson sampling²¹ schemes were proposed and demonstrated¹⁴. Yet, so far, all the previous quantum optical boson-sampling machines⁹⁻¹⁷ have demonstrated only up to three single photons with arbitrary input configurations and 4-6 photons in special Fock states, and the obtained sampling rates were several orders of magnitudes too low to even outperform some of the earliest classical computers.

Indistinguishable single photons

Scaling up boson-sampling to large number of photons and with high sampling rates represents a non-trivial experimental challenge. Importantly, it requires high-performance single quantum emitters²²⁻²⁴ that can deterministically produce one and only one photon under each pulsed excitation. The generated photons must simultaneously have high single-photon purity (that is, the multi-photon probability should be vanishingly small), high indistinguishability (that is, photons are quantum mechanically identical to each other), and high collection efficiency into a single spatial mode²⁵⁻²⁷. These three key features are compatibly combined in our experiment using pulsed *s*-shell resonant excitation²⁸ of a single self-assembled InAs/GaAs quantum dot embedded inside a micropillar cavity²⁹⁻³¹ (see Fig.1 and Supplementary Information).

At π pulse excitation with a repetition rate of 76 MHz, the quantum dot-micropillar emits ~ 25.6 million polarized, resonance fluorescence single photons per second at the output of a single-mode fiber, of which ~ 6.5 million are eventually detected on a silicon single-photon detector. Considering the detector dead time of ~ 42 ns, the actual count rate should be corrected to 9 MHz (Fig. 2a). This is the brightest single-photon source reported in all physical systems to date, which are directly used—without any spectral

filtering—for the photon correlation and interference measurements, and for boson sampling. We measure its second-order correlation, and observed $g^2(0) = 0.027(1)$ at zero time delay, which confirmed the high purity of the single-photon Fock state. We perform Hong-Ou-Mandel interference as a function of the emission time separation between two single photons³¹. With a time separation of 13 ns and 14.7 μ s, photon indistinguishabilities of 0.939(3) and 0.900(3) are measured, respectively (see Fig. 2b and Supplementary Information). Thanks to the pulsed resonant excitation method that eliminates dephasings and time jitter²⁸, we obtain long streams near-transform-limited single photons that are sufficient for multi-photon experiments on a semiconductor chip for the first time.

Efficient multi-photon source

Next, we de-multiplex the single-photon stream into different spatial modes using fast optical switches that consist of Pockels cells (with a transmission rate >99% and extinction ratio >100:1) and polarizing beam splitters (with an extinction ratio >1200:1). The Pockels cells, synchronized to the pulsed laser and operated at 0.76 MHz with a rising time of 8 ns, convert the single-photon pulse train into 3, 4, or 5 separate beams (see Supplementary Information and Fig. S5). The largest time separation between two de-multiplexed photons is $\sim 1.05 \mu$ s (80 pulses), where the photon indistinguishability remains 0.923 (Fig. 2b).

To ensure that these pulses arrive simultaneously at a multi-mode interferometer, optical fibers of different lengths and translation stage are used to finely adjust their arrival time. The average efficiency of the optical switches is $\sim 84.5\%$, which was mainly due to the coupling efficiency and propagation loss in the optical fibers. The efficiency can be improved in the future using faster Pockels cells (see Supplementary Information). Thus, we eventually obtain five separate single-photon sources with end-user efficiencies of about 28.4%. Note the active de-multiplexing method eliminates the common technical overhead for overcoming the inhomogeneity of independent self-assembled quantum dots to build many identical sources.

Ultra-low-loss photonic circuit

Another important ingredient for reliable and fast boson-sampling is a multi-mode interferometric linear optical network that is phase stable, has high transmission rate, and can implement a Haar-random unitary matrix. While the previously demonstrated waveguide-based photonic chips showed promise for large-scale integration¹⁰⁻¹⁶, the coupling and propagation loss in these chips seriously limited the overall efficiencies to ~30% so far (see Supplementary Information Table S1).

Here, we put forward a new circuit design that simultaneously combines the stability, matrix randomness, and ultra-low transmission loss. As shown in Fig. 1 (see also Fig. S6), a 9×9 mode interferometer is constructed with a bottom-up approach, from individual tiny trapezoid, each optically coated with polarization-dependent beam splitting ratios (Supplementary Information). This network consists of 36 beam splitters and 9 mirrors, and implements a near-unitary transformation to input state (Fig. 2c, d). Thanks to the antireflection coating, the overall transmission efficiency (from input to output) is measured to be above 99%. By Mach-Zehnder-type coherence measurements, the spatial-mode overlap is determined to better than 99.9%. The interferometer is housed on a temperature-stabilized baseplate, and remains stable at least for weeks (for a test, see Fig. S7). Such a design can be further improved³² and scaled up to reasonably larger dimensions, which can be sufficient for the near-term goal of demonstrating quantum supremacy through boson sampling.

Experimental results and validation

We send three, four, and five single photons into the 9-mode interferometer, and measure the output multi-photon events, as shown in Fig. 3. We use nine silicon single-photon avalanche detectors (efficiency ~32%), one in each output of the interferometer, to register the no-collision (one photon per output-mode) events, which have 84, 126, and 126 different output distributions for the 3-, 4-, and 5-boson sampling, respectively. A total of 446084 three-photon events (Fig. 3a), 36261 four-photon events (Fig. 3b), and 11660 five-photon events (Fig. 3c) are obtained in accumulation time of 90s, 240s,

and 2900s, respectively. The obtained data (solid bar, denoted as q_i) are plotted together with ideal probability distribution (empty bar, denoted as p_i) in Fig. 3. We quantify the match between these two sets of distributions using the measure of similarity, defined as $F = \sum_i \sqrt{p_i q_i}$, and the measure of distance, defined as $D = (1/2) \sum_i |p_i - q_i|$. From the data in Fig. 3, we can calculate similarities of 0.984(1), 0.979(5), and 0.973(9), and distanness of 0.125(1), 0.141(3), and 0.178(5) for the 3-, 4-, and 5-boson sampling, respectively.

For a large-scale boson-sampling device, not only the calculation of its outcome, but also a full certification of the outcome is strongly conjectured to be intractable for classical computation. There have been proposals³³⁻³⁵ and demonstrations^{15,16} for validating boson-sampling that can provide supporting or circumstantial evidence for the correct operation of this protocol. In our work, we first employ Bayesian analysis³⁴ to rule out uniform distribution (Fig. 4a). With only ~20 events, we can reach a confidence level of 99.8% that these outcomes are from genuine boson-samplers. Another possible hypothesis is using distinguishable single photons (classical particles) or spatial-mode mismatched interferometers, which should be excluded by applying standard likelihood ratio test³⁵. Figure 4b shows an increasing difference between solid (indistinguishable bosons) and dotted lines (distinguishable bosons) as experimental events increasing, and thus the distinguishable hypothesis is ruled out with only ~50 events (see Supplementary Information).

Conclusion and outlook

Owing to our development of the high-efficiency source of highly indistinguishable single photons and ultra-low-loss photonic circuits, the experiment demonstrated 3-boson sampling rate of 4.96 KHz is ~27,000 times faster than the best previous experiments using SPDC⁹⁻¹⁶, and ~24,000 times faster than the recent work¹⁷ using passive demultiplexing (thus intrinsically inefficient) of quantum-dot single photons using incoherent excitation that limited the photon indistinguishability to 52%-64%. Meanwhile, we achieve the first 4- and 5-boson sampling using single-photon Fock

state—which were formidable challenges before—and obtain high sampling rates of 151 Hz and 4 Hz, respectively. These multi-photon boson-sampling machines have also reached a computational complexity that can race against early classical computers. Under the specific racing rule in ref. 5, 9, 10, we could compare the required time for obtaining one output sample using the quantum machines with the simulated time for calculating one permanent using the published data of the early classical computers (see Supplementary Information). As shown in Table SII, the quantum photonic machines are provably faster for the boson-sampling task than ENIAC and TRADIC, the first electronic computer and transistorized computer.

Our work has demonstrated a clear, realistic pathway to build boson-sampling machines with many photons and fast rates. Using superconducting nanowire single-photon detectors^{36,37} with reported efficiency of ~95% and antireflection optical coating, one can straightforwardly increase the 3-, 4-, and 5-boson sampling rates to 130 KHz, 12 KHz, and 1 KHz, respectively, and implement 14-boson-sampling with a count rate of 5/h (see Supplementary Information). A remaining challenge is to remove the cross-polarization in the confocal setup—used to extinguish the laser background—which reduced the single-photon source efficiency by half. Future work will focus on deterministic dot-micropillar coupling³⁸ and developing side excitation³⁹ to boost the single-photon source efficiency to over 74%, in which case we can expect 20-boson sampling rate of ~130/h, and an increasing quantum advantage over classical computation for larger number of photons.

References:

1. Ladd, T. D. et al. Quantum computers. *Nature* 464, 45-53 (2010).
2. Pan, J.-W. et al. Multiphoton entanglement and interferometry. *Rev. Mod. Phys.* 84, 777-838 (2012).
3. Barends, R. et al. Superconducting quantum circuits at the surface code threshold for fault tolerance. *Nature* 508, 500-503 (2014).

4. Monz, T. et al. Realization of a scalable Shor algorithm. *Science* 351, 1068-1070 (2016).
5. Aaronson, S. & Arkhipov, A. The computational complexity of linear optics. In *Proceedings of the 43rd Annual ACM Symposium on Theory of Computing* 333-342 (ACM, New York, 2011).
6. Kok, P. et al. Linear optical quantum computing with photonic qubits. *Rev. Mod. Phys.* 79, 135-174 (2007).
7. Rohde, P. R. & Ralph, T. C. Error tolerance of boson-sampling model for linear optical quantum computing. *Phys. Rev. A* 85, 022332 (2012).
8. Wu, J.-J. et al. Computing permanents for boson sampling on Tianhe-2 supercomputer. Preprint at <https://arxiv.org/abs/1606.05836> (2016).
9. Broome, M. A. et al. Photonic boson sampling in a tunable circuit. *Science* 339, 794-798 (2013).
10. Spring, J. B. et al. Boson sampling on a photonic chip. *Science* 339, 798-801 (2013).
11. Tillmann, M. et al. Experimental boson sampling. *Nat. Photon.* 7, 540-544 (2013).
12. Crespi, A. et al. Integrated multimode interferometers with arbitrary designs for photonic boson sampling. *Nat. Photon.* 7, 545-549 (2013).
13. Carolan, J. et al. Universal linear optics. *Science* 349, 711-716 (2015).
14. Bentivegna, M. et al. Experimental scattershot boson sampling. *Sci. Adv.* 1, e1400255 (2015).
15. Carolan, J. et al. On the experimental verification of quantum complexity in linear optics. *Nat. Photon.* 8, 621-626 (2014).
16. Spagnolo, N. et al. Experimental validation of photonic boson sampling. *Nat. Photon.* 8, 615-620 (2014).
17. Loredano, J. C. et al. Boson sampling with single photon Fock states from a bright solid-state source. Preprint at <https://arxiv.org/abs/1603.00054> (2016)
18. Kwiat, P. G. et al. New high-intensity source of polarization-entangled photon pairs.

Phys. Rev. Lett. 75, 4337-4341 (1995).

19. Pittman, T., Jacobs, B. & Franson, J. Single photons on pseudodemand from stored parametric down-conversion. Phys. Rev. A 66, 042303 (2002).

20. Kaneda, F. et al. Time-multiplexed heralded single-photon source. Optica 2, 1010-1013 (2015).

21. Lund, A. P. et al. Boson sampling from a Gaussian state. Phys. Rev. Lett. 113, 100502 (2014).

22. Lounis, B. & Orrit, M. Single photon sources. Rep. Prog. Phys. 68, 1129-1179 (2005).

23. Michler, P. et al. A quantum dot single-photon turnstile device. Science 290, 2282-2285 (2000).

24. Santori, C., Fattal, D., Vučković, J., Solomon, G. S. & Yamamoto, Y. Indistinguishable photons from a single photon device. Nature 419, 594-597 (2002).

25. Tillmann, M. et al. Generalized multiphoton quantum interference. Phys. Rev. X 5, 041015 (2015).

26. Shchesnovich, V. S. Partial indistinguishability theory of multiphoton experiments in multiport devices. Phys. Rev. A 91, 013844 (2015).

27. Tichy, M. C. Sampling of partially distinguishable bosons and the relation to multidimensional permanent. Phys. Rev. A 91, 022316 (2015).

28. He, Y.-M. et al. On-demand semiconductor single-photon source with near-unity indistinguishability. Nat. Nanotech. 8, 213-217 (2013).

29. Ding, X. et al. On-demand single photons with high extraction efficiency and near-unity indistinguishability from a resonantly driven quantum dot in a micropillar. Phys. Rev. Lett. 116, 020401 (2016).

30. Somaschi, N. et al. Near-optimal single-photon sources in the solid state. Nat. Photon. 10, 340-345 (2016).

31. Wang, H. et al. Near-transform-limited single photons from an efficient solid-state

- quantum emitter. *Phys. Rev. Lett.* 116, 213601 (2016).
32. Clements, W. R., Humphreys, P. C., Metcalf, B. J., Kolthammer, W. S., Walmsley, I. A. An optimal design for universal quantum multiport interferometers. Preprint at <https://arxiv.org/abs/1603.08788> (2016).
 33. Aaronson, S. & Arkhipov, A. Bosonsampling is far from uniform. *Quant. Inf. Comp.* 14, 1383-1432 (2014).
 34. Bentivegna, M. et al. Bayesian approach to boson sampling validation. *Int. J. Quant. Inf.* 12, 1560028 (2014).
 35. Cover, T. M. & Thomas, J. A. *Elements of Information Theory* (John Wiley & Sons, 2006).
 36. Lita, A. E., Miller, A. J., & Nam, S. W. Counting near-infrared single-photons with 95% efficiency. *Opt. Express* 16, 3032-3040 (2008).
 37. Zadeh, I. E. et al. Single photon detectors combining near unity efficiency, ultra-high detection-rates, and ultra-high time resolution. Preprint at <https://arxiv.org/abs/1611.03245> (2016).
 38. Unsleber, S., et al. Highly indistinguishable on-demand resonance fluorescence photons from a deterministic quantum dot micropillar device with 74% extraction efficiency. *Opt. Express* 24, 8539-8546 (2016).
 39. Muller, A. et al. Resonant fluorescence from a coherent driven semiconductor quantum dot in a cavity. *Phys. Rev. Lett.* 99, 187402 (2007).

Acknowledgements:

We thank S. Aaronson, B. Sanders, and P. Rohde for helpful discussions. This work was supported by the National Natural Science Foundation of China, the Chinese Academy of Sciences, the National Fundamental Research Program, and the State of Bavaria.

Author contributions:

C.-Y.L. and J.-W.P. conceived and designed the experiment, C.S., M.K., and S.H. grew and fabricated the quantum dot samples. H.W., Y.H., Y.-H.L., Z.-E.S., B.L., H.-L.H., X.D., M.-C.C., C.L., J.Q., J.-P. L., Y.-M.H., C.S., M.K., C.-Z.P., S.H., and C.-Y.L. performed the experiment, S.H., C.-Y. L., and J.-W.P. analyzed the experimental data, and C.-Y.L. and J.-W.P. wrote the paper.

Author Information:

The authors declare no competing financial interests. Correspondence and requests for materials should be addressed to C.-Y.L. (cylu@ustc.edu.cn) or J.-W.P. (pan@ustc.edu.cn).

Data availability:

The data that support the plots within this paper and other findings of this study are available from the corresponding author upon reasonable request.

Figure captions:

Figure 1 | Experimental setup for multi-photon boson-sampling. The setup includes four key parts: the single-photon device, de-multiplexers, ultra-low-loss photonic circuit, and detection. The single-photon device is a single InAs/GaAs quantum dot coupled to a 2- μm diameter micropillar cavity, which yields a Purcell factor of 7.63(23) at resonance. The quantum dot is coherently pumped by a picosecond laser. A confocal microscope is operated in a cross-polarization configuration to extinguish laser background. The resonance fluorescence single photons collected into a single-mode fiber are sent to active de-multiplexers, which consist of Pockels cells and polarizing beam splitters, and separated into five spatial modes. The five photons are then fed into a tailor-made ultra-low-loss photonic circuit that consists of 36 beam splitters. Finally, the output out of the interferometer are measured by nine single-photon detectors and the multi-photon coincidence are analyzed by a time-to-digit converter (TDC).

Figure 2 | The single photon source and interferometer for boson-sampling. a,

Observed Rabi oscillation by pulsed resonant excitation of the quantum dot. The blue dots are directly measured by silicon detectors, whereas the red dots are corrected by the dead time of the detectors. The single-photon counts reach maximum at the π pulse power, which is 1.6 nW. **b**, The measured photon indistinguishability drops slightly from 0.939(3) at 13 ns to a plateau of 0.900(3) at >10 μ s separation, fitted with a decaying time constant of 2.1 μ s, assuming non-Markovian noise model. The blue arrow indicates the regime in our current work where two photons are maximally separated by a time of 1.05 μ s due to de-multiplexing. The error bars denote one standard deviations, deduced from propagated Poissonian counting statistics of the raw photon detection events. **c**, **d**, Measured elements (**c**, amplitude and **d**, phase) of the unitary transformation of the optical network.

Figure 3 | Experimental results for the (a) 3-, (b) 4-, and (c) 5-boson sampling. The measured relative frequencies of all no-collision output combinations, denoted by (i, j, \dots) where there is one photon detected in each output mode i, j, \dots . The solid bars are the normalized coincidence rate of different output distribution. The empty bars are theoretical calculations in the ideal case. The error bar is one standard deviation from Poissonian counting statistics.

Figure 4 | Validating boson sampling results. The open points in **a** and the dotted lines in **b** are tests applied on simulated data generated from the two alternative hypotheses, sampling from a uniform distribution and distinguishable particles, respectively. In both **a** and **b**, the solid points and solid lines are tests applied on the experimental data. A counter is updated for every event and a positive value validates the data being obtained from a genuine boson sampler. **a**, Application of the Bayesian analysis to test against uniform distribution. **b**, Discrimination of the data from a distinguishable sampler using standard likelihood ratio test.

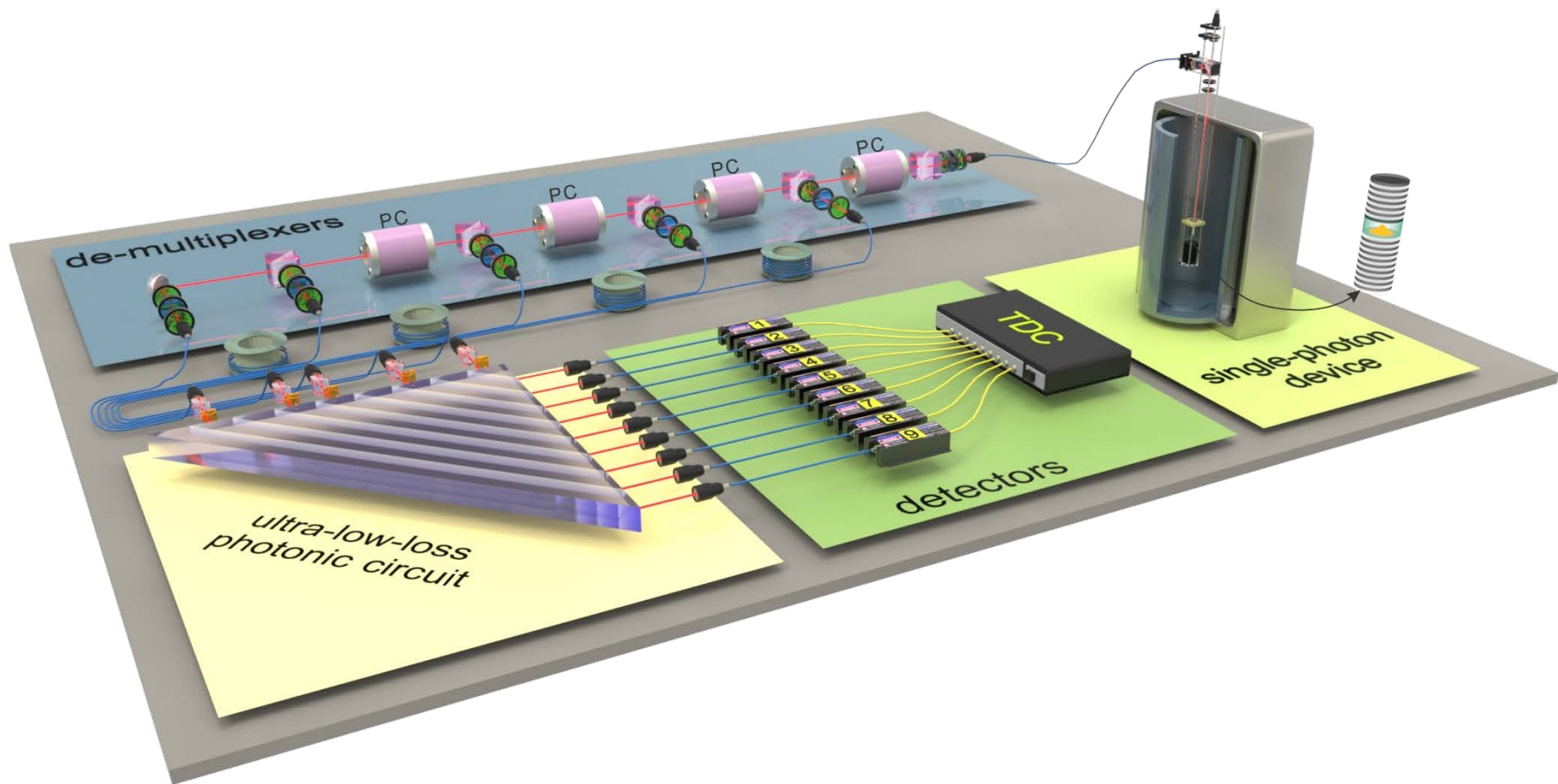


Figure 1

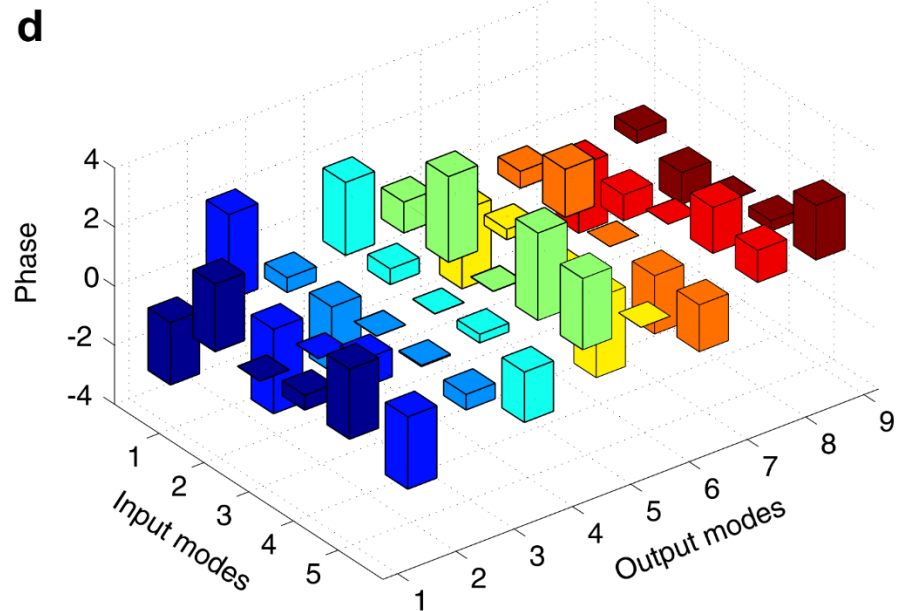
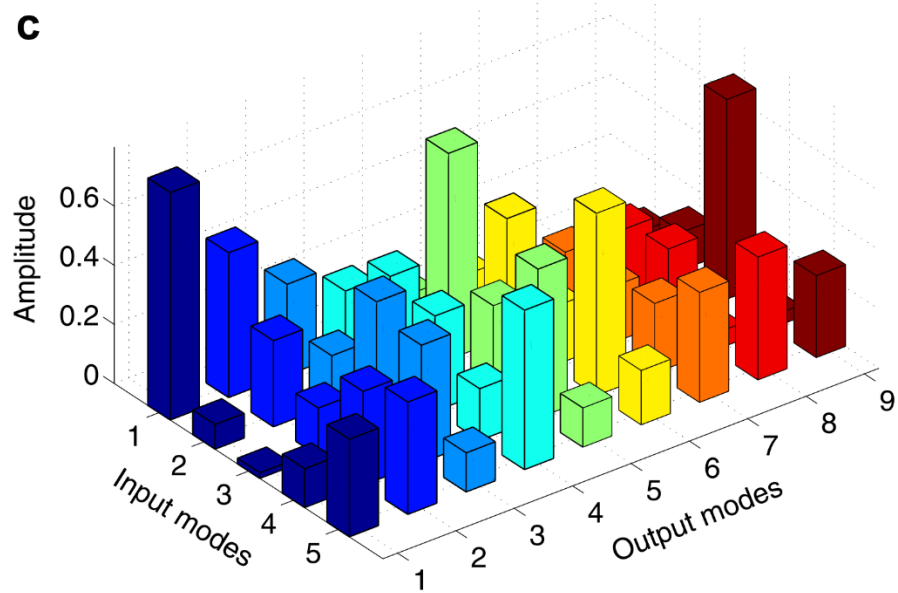
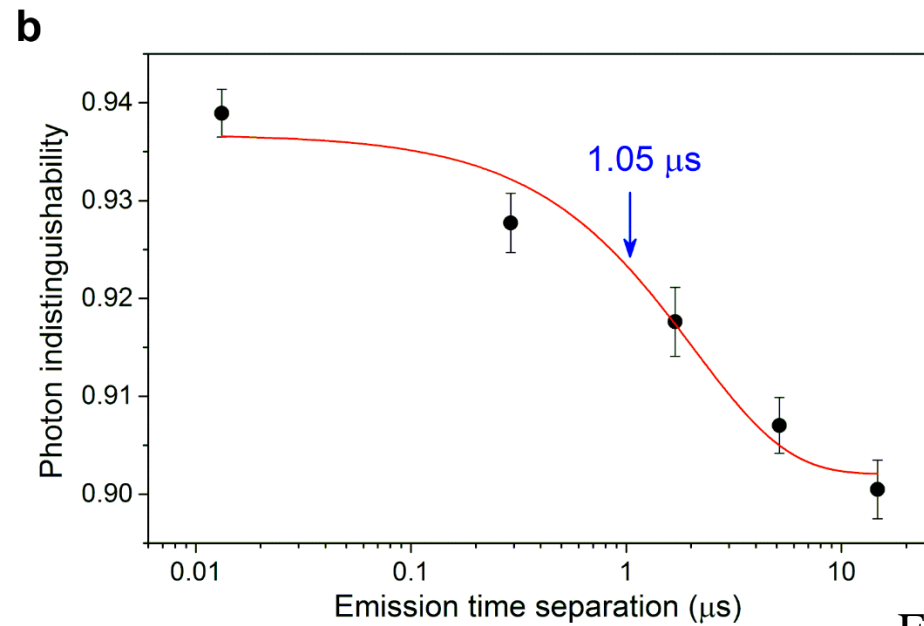
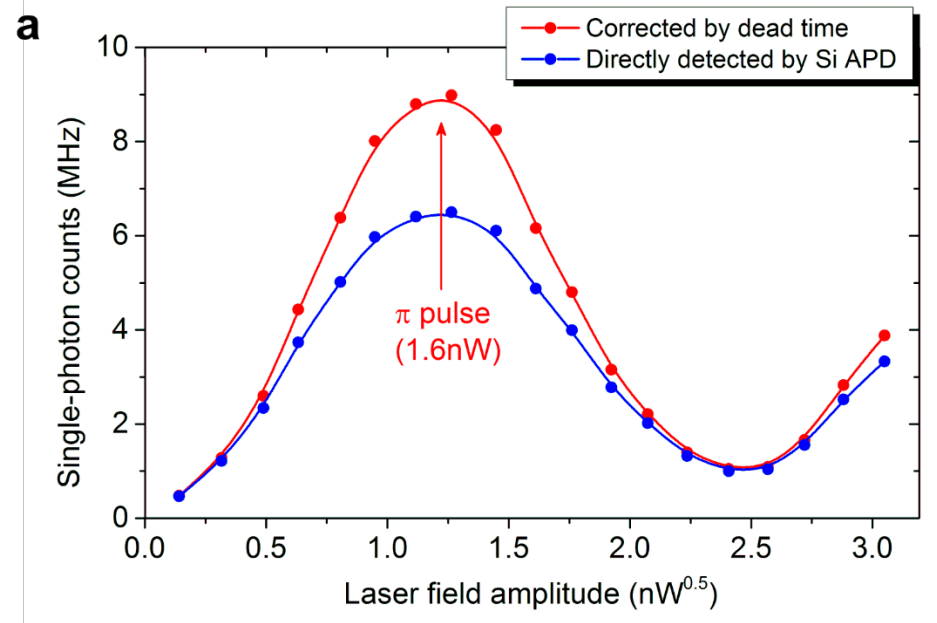


Figure 2

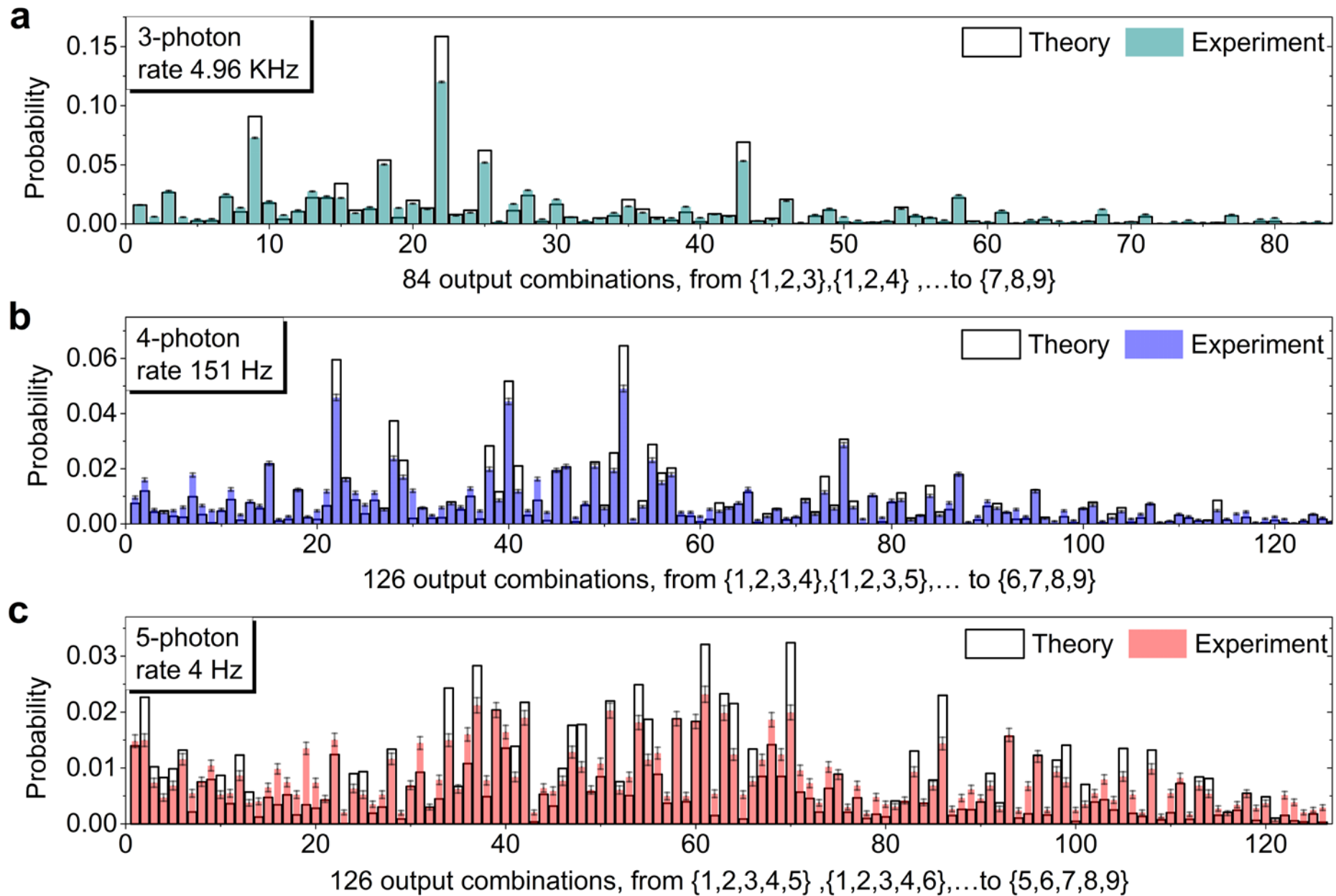


Figure 3

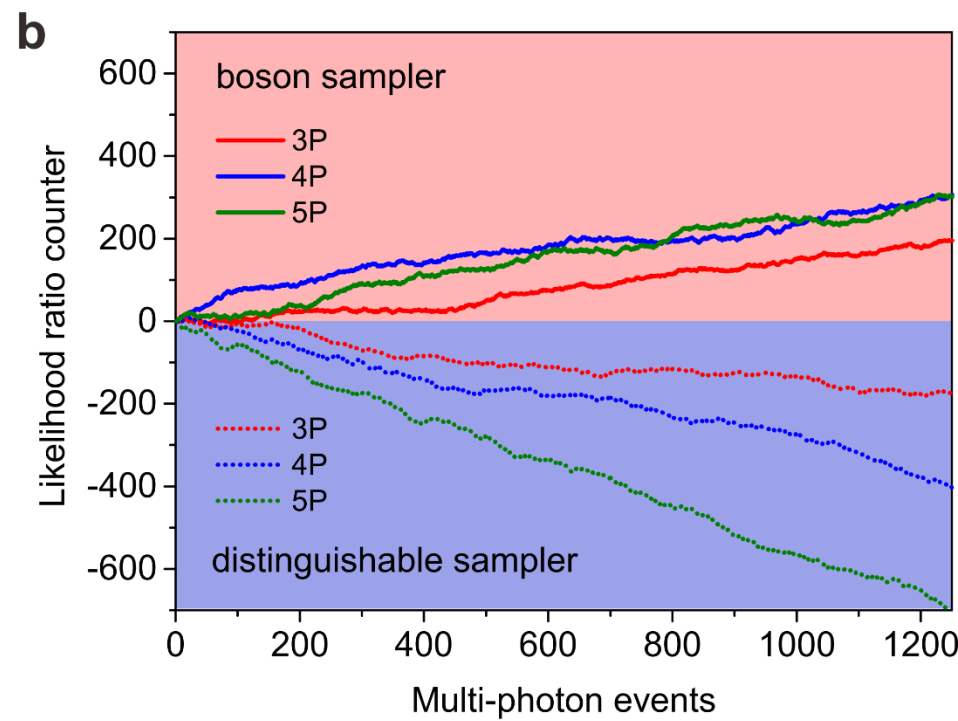
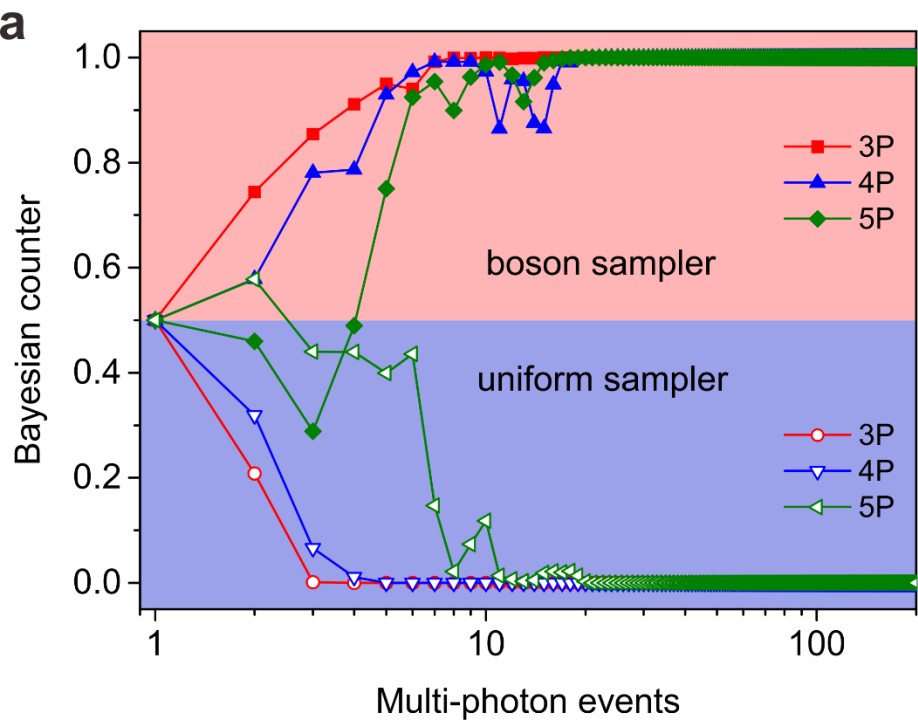


Figure 4